Energy spectra of narrow- and zero-gap-semiconductor quantum dots

2000 J. Phys.: Condens. Matter 12 7923

(http://iopscience.iop.org/0953-8984/12/36/307)

J. Phys.: Condens. Matter **12** (2000) 7923–7932. Printed in the UK PII: S0953-8984(00)12369-0

Energy spectra of narrow- and zero-gap-semiconductor quantum dots

F M Gashimzade, A M Babaev and M A Bagirov

Institute of Physics, Azerbaijan Academy of Sciences, H Cavid Avenue, 33, 370143, Baku, Azerbaijan

E-mail: conmat@artel.net.az

Received 6 March 2000, in final form 15 June 2000

Abstract. The size dependence of the spectra of free carriers in A^3B^5- and A^2B^6-type-semiconductor spherical quantum dots is studied. The advantage of a universal method for obtaining equations that are invariant under the transformations of the rotations group, which directly yields a system of equations for the radial functions for any number of bands considered, is demonstrated. The calculated energy eigenstates of the spherical InAs quantum dot and quantum dots based on zero- and narrow-gap semiconductors of the HgTe and $Cd_{1-x}Hg_xTe$ ($x < 0.16$) types are presented.

1. Introduction

To describe the spectra of free carriers in A^3B^5- and A^2B^6-type-semiconductor quantum dots, the spherically symmetric Luttinger Hamiltonian has been used [1–5].

In reference [3], a new formalism for determining energy eigenstates of spherical quantum dots and cylindrical quantum wires in the multiple-band envelope-function approximation was described. The bound states were studied for the conduction band and coupled light and heavy holes, as a function of the radius of the $GaAs/Al_xGa_{1-x}As$ quantum dot. Conduction band–valence band coupling was shown to be critical in a 'type-II' InAs/GaSb quantum dot. Implications of the band-coupling effects for optical matrix elements for quantum wires and dots were discussed.

The size dependence of the electron and hole quantum size levels in spherical semiconductor nanocrystals was studied in reference [4]. In that work, an analytical theory of the quantum size levels within a spherical eight-band Pidgeon and Brown model, which takes into account both the coupling of conduction and valence bands and the complex structure of the valence band in nanocrystals with an infinite potential barrier, was developed. The calculated level structures for narrow-gap InSb, moderate-gap CdTe, and wide-gap CdS nanocrystals were presented.

In reference [5], the electronic structure of pyramid-shaped InAs/GaAs quantum dots was calculated.

Note that in all of the above-cited works, to make the calculations, different models of the band structure were used. However, there is a universal method for obtaining equations that are invariant under the transformations of the rotation group [6, 7], which directly gives a system of equations for the radial functions for any number of bands considered. Using this method, it is possible also to take into account higher conduction bands.

0953-8984/00/367923+10$30.00

2. Method of calculation

In this paper we shall demonstrate the advantage of the above-mentioned universal method for the cases of InAs and HgTe quantum dots. In figure 1 the bulk structures of InAs-type (figure 1(a)) and HgTe-type (figure 1(b)) semiconductors near the Γ point are shown. In the cases considered, the band gap E_g and spin–orbit splitting Δ are of the same order. For this reason, it is important to take into account a conduction band, which we shall label with double indices (1/2; 0), the heavy- and light-hole bands (3/2; 1), and the spin–orbit-splitting band (1/2; 1). To obtain a finite heavy-hole effective mass, it is necessary to include the higher conduction bands (5/2; 2) and (3/2; 2) also. The first index characterizes the weight of the irreducible representation and the second one indicates the subspace with the same weight. We have chosen indices for the states which clearly show that they are created from the corresponding s, p, and d states. In order to give a physical meaning to the equations, we consider the coefficients connecting s, p, and d states, namely, $\tau = 0$, $\tau = 1$, and $\tau = 2$, respectively, to be nonzero, where τ is the number of the subspace.

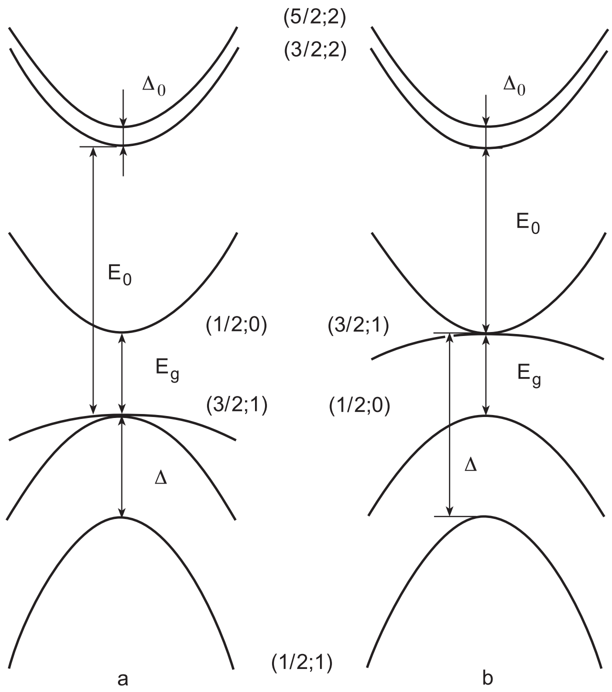

Figure 1. The bulk structure of InAs-type (a) and HgTe-type (b) semiconductors near the Γ point.

Thus according to [6, 7] we should have the following system of first-order ordinary differential equations for the radial functions†:

$$\frac{-\mathrm{i}a}{2(E-E_g)}\left[\frac{\mathrm{d}}{\mathrm{d}r}+\frac{1\mp(l_0+\frac{1}{2})}{r}\right]f_3^{\mp} - \frac{\mathrm{i}\sqrt{2}b}{E-E_g}\left\{\left[\frac{\mathrm{d}}{\mathrm{d}r}+\frac{5\pm(l_0+\frac{1}{2})}{2r}\right]f_2^{\pm}+\frac{\alpha}{r}f_1^{\mp}\right\}+f_0^{\mp}=0 \qquad (1)$$

† There are obvious misprints in the equations of Gelfand *et al* [6] and Lyubarsky [7]. In particular, in the ninth term in equation (18) in section 9 in [6], l should be replaced by $l+2$, and in equation (60.12) in [7], the sign before the term containing a derivative should be changed.

$$\frac{\mathrm{i}\sqrt{2}b}{E}\frac{\alpha}{r}f_0^{\pm} - \frac{\mathrm{i}c}{E}\left[\frac{3}{2}\left(\frac{\mathrm{d}}{\mathrm{d}r}+\frac{1}{r}\right)f_4^{\mp}+\frac{\alpha}{r}f_5^{\mp}\right]$$
$$-\frac{\mathrm{i}e}{E}\left\{\frac{\sqrt{5}}{2}\frac{\sqrt{(l_0+\frac{5}{2})(l_0-\frac{3}{2})}}{r}f_6^{\pm}+\sqrt{\frac{2}{3}}\frac{\alpha}{r}f_8^{\pm}+2\left(\frac{\mathrm{d}}{\mathrm{d}r}+\frac{7}{2r}\right)f_7^{\pm}\right\}+f_1^{\pm}=0 \tag{2}$$

$$-\frac{\mathrm{i}\sqrt{2}b}{E}\left[\frac{\mathrm{d}}{\mathrm{d}r}-\frac{1\pm(l_0+\frac{1}{2})}{2r}\right]f_0^{\pm}-\frac{\mathrm{i}c}{E}\left\{\frac{1}{2}\left[\frac{\mathrm{d}}{\mathrm{d}r}+\frac{1\mp(2l_0+1)}{r}\right]f_5^{\mp}-\frac{\alpha}{r}f_4^{\mp}\right\}$$
$$-\frac{\mathrm{i}e}{E}\left\{2\frac{\alpha}{r}f_7^{\pm}+\sqrt{6}\left[\frac{\mathrm{d}}{\mathrm{d}r}+\frac{7\pm(l_0+\frac{1}{2})}{2r}\right]f_8^{\pm}\right\}+f_2^{\pm}=0 \tag{3}$$

$$\frac{-\mathrm{i}a}{2(E+\Delta)}\left[\frac{\mathrm{d}}{\mathrm{d}r}+\frac{1\mp(l_0+\frac{1}{2})}{r}\right]f_0^{\mp}-\frac{\mathrm{i}\sqrt{2}d}{E+\Delta}\left\{\left[\frac{\mathrm{d}}{\mathrm{d}r}+\frac{5\pm(l_0+\frac{1}{2})}{2r}\right]f_5^{\pm}+\frac{\alpha}{r}f_4^{\pm}\right\}+f_3^{\pm}=0 \tag{4}$$

$$-\frac{\mathrm{i}\sqrt{2}d}{E-E_0}\frac{\alpha}{r}f_3^{\pm}-\frac{\mathrm{i}c}{E-E_0}\left\{\frac{3}{2}\left(\frac{\mathrm{d}}{\mathrm{d}r}+\frac{1}{r}\right)f_1^{\mp}+\frac{\alpha}{r}f_2^{\mp}\right\}+f_4^{\pm}=0 \tag{5}$$

$$-\frac{\mathrm{i}\sqrt{2}d}{E-E_0}\left[\frac{\mathrm{d}}{\mathrm{d}r}-\frac{1\pm(l_0+\frac{1}{2})}{2r}\right]f_3^{\pm}$$
$$-\frac{\mathrm{i}c}{E-E_0}\left\{\left[\frac{\mathrm{d}}{\mathrm{d}r}-\frac{1\mp(2l_0+1)}{r}\right]f_2^{\mp}-\frac{\alpha}{r}f_1^{\mp}\right\}+f_5^{\pm}=0 \tag{6}$$

$$-\frac{\mathrm{i}\sqrt{5}e}{E-E_0-\Delta_0}\frac{\sqrt{(l_0+\frac{5}{2})(l_0-\frac{3}{2})}}{r}f_1^{\pm}+f_6^{\pm}=0 \tag{7}$$

$$-\frac{\mathrm{i}e}{E-E_0-\Delta_0}\left[2\left(\frac{\mathrm{d}}{\mathrm{d}r}-\frac{3}{2r}\right)f_1^{\pm}-\frac{2\alpha}{r}f_2^{\pm}\right]+f_7^{\pm}=0 \tag{8}$$

$$-\frac{\mathrm{i}e}{E-E_0-\Delta_0}\left[\sqrt{6}\left[\frac{\mathrm{d}}{\mathrm{d}r}-\frac{3\pm(l_0+\frac{1}{2})}{2r}\right]f_2^{\pm}-\sqrt{\frac{2}{3}}\frac{\alpha}{r}f_1^{\pm}\right]+f_8^{\pm}=0. \tag{9}$$

Here the following designations are used:

$$\begin{aligned}
f_0^{\pm} &= f^{l_0}_{\frac{1}{2},\frac{1}{2},0} \pm f^{l_0}_{\frac{1}{2},-\frac{1}{2},0} & f_5^{\pm} &= f^{l_0}_{\frac{3}{2},\frac{1}{2},2} \pm f^{l_0}_{\frac{3}{2},-\frac{1}{2},2}\\
f_1^{\pm} &= f^{l_0}_{\frac{3}{2},\frac{3}{2},1} \pm f^{l_0}_{\frac{3}{2},-\frac{3}{2},1} & f_6^{\pm} &= f^{l_0}_{\frac{5}{2},\frac{5}{2},2} \pm f^{l_0}_{\frac{5}{2},-\frac{5}{2},2}\\
f_2^{\pm} &= f^{l_0}_{\frac{3}{2},\frac{1}{2},1} \pm f^{l_0}_{\frac{3}{2},-\frac{1}{2},1} & f_7^{\pm} &= f^{l_0}_{\frac{5}{2},\frac{3}{2},2} \pm f^{l_0}_{\frac{5}{2},-\frac{3}{2},2}\\
f_3^{\pm} &= f^{l_0}_{\frac{1}{2},\frac{1}{2},1} \pm f^{l_0}_{\frac{1}{2},-\frac{1}{2},1} & f_8^{\pm} &= f^{l_0}_{\frac{5}{2},\frac{1}{2},2} \pm f^{l_0}_{\frac{5}{2},-\frac{1}{2},2}\\
f_4^{\pm} &= f^{l_0}_{\frac{3}{2},\frac{3}{2},2} \pm f^{l_0}_{\frac{3}{2},-\frac{3}{2},2}
\end{aligned} \tag{10}$$

as well as

$$
\begin{aligned}
&\frac{C^{0,1}_{1/2,1/2}}{\mathrm{i}\chi} = \frac{\mathrm{i}a}{E-E_g} \qquad &&\frac{C^{1,0}_{1/2,1/2}}{\mathrm{i}\chi} = \frac{\mathrm{i}a}{E+\Delta}\\
&\frac{C^{0,1}_{1/2,3/2}}{\mathrm{i}\chi} = \frac{\mathrm{i}b}{E-E_g} \qquad &&\frac{C^{1,0}_{1/2,1/2}}{\mathrm{i}\chi} = \frac{\mathrm{i}b}{E}\\
&\frac{C^{1,2}_{3/2,3/2}}{\mathrm{i}\chi} = \frac{\mathrm{i}c}{E} \qquad &&\frac{C^{2,1}_{3/2,3/2}}{\mathrm{i}\chi} = \frac{\mathrm{i}c}{E-E_0}\\
&\frac{C^{1,2}_{1/2,3/2}}{\mathrm{i}\chi} = \frac{\mathrm{i}d}{E+\Delta} \qquad &&\frac{C^{2,1}_{3/2,1/2}}{\mathrm{i}\chi} = \frac{\mathrm{i}d}{E-E_0}\\
&\frac{C^{1,2}_{3/2,5/2}}{\mathrm{i}\chi} = \frac{\mathrm{i}e}{E} \qquad &&\frac{C^{2,1}_{5/2,3/2}}{\mathrm{i}\chi} = \frac{\mathrm{i}e}{E-E_0-\Delta_0}
\end{aligned}
\tag{11}
$$

where E_g is the energy of the bottom of the conduction band, Δ is the spin–orbit-splitting energy, and E_0 and $E_0 + \Delta_0$ are the energies of the higher conduction bands, responsible for the finite heavy-hole mass. The parameters a, b, c, d, and e are matrix elements taking into consideration the interactions between the conduction and valence bands. Quantities like $C^{0,1}_{1/2,1/2}$, $f^{l_0}_{1/2,1/2,0}$ etc, and χ were determined by Gelfand *et al* [6]. The system of equations (1)–(9) have been rewritten so as to separate the independent solutions ('even' and 'odd').

3. The energy spectrum

Excluding from the system (1)–(9) the functions $f_4^{\pm}$, $f_5^{\pm}$, $f_6^{\pm}$, $f_7^{\pm}$, and $f_8^{\pm}$, we obtain a system of equations describing the conduction band, and light- and heavy-hole bands, as well as the spin–orbit-splitting band.

From the solvability condition for the system of equations (1)–(9), we find that the equation describing the spectra of electrons, light-hole bands, and spin–orbit-splitting bands has the form

$$
\left[1 - \frac{a^2k^2}{4(E+\Delta)(E-E_0)} - \frac{2d^2k^2}{(E+\Delta)(E-E_0)}\right]\left[1 - \frac{6e^2k^2}{E(E-E_0-\Delta_0)}\right] + \frac{(ac/4-2bd)^2k^4}{E(E-E_g)(E+\Delta)(E-E_0)} - \frac{2b^2k^2}{E(E-E_g)} - \frac{c^2k^2}{4E(E-E_0)} = 0. \tag{12}
$$

The spectrum of the heavy-hole band is defined by the equation

$$
1 - \frac{9}{4}\frac{c^2k_h^2}{E(E-E_0)} - \frac{4e^2k_h^2}{E(E-E_0-\Delta_0)} = 0. \tag{13}
$$

The parameters a, b, c, d, and e can be expressed through effective masses. Equations (12) and (13) for $k = 0$ and $k_h = 0$ have the following eigenvalues (for InAs):

$$
E_n = E_g \qquad E_{hh} = 0 \qquad E_{lh} = 0 \qquad E_{sh} = -\Delta
$$

corresponding to the conduction band, heavy- and light-hole bands, and spin–orbit-splitting band. Putting this zero solution into equations (12) and (13) for small k, we obtain the spectrum for the parabolic approximation. Then for the effective mass we find

$$\begin{aligned}
\frac{\hbar^2}{2m_n} &= \frac{2b^2}{E_g} + \frac{1}{4}\frac{a^2}{E_g + \Delta} \\
\frac{\hbar^2}{2m_{hh}} &= \frac{9c^2}{4E_0} + \frac{4e^2}{E_0 + \Delta_0} \\
\frac{\hbar^2}{2m_{lh}} &= \frac{2b^2}{E_g} + \frac{c^2}{4E_0} + \frac{6e^2}{E_0 + \Delta_0} \\
\frac{\hbar^2}{2m_{sh}} &= \frac{1}{4}\frac{a^2}{E_g + \Delta} + \frac{2d^2}{E_0 + \Delta_0}
\end{aligned} \tag{14}$$

where m_n, m_{hh}, m_{lh}, and m_{sh} are the effective masses of the electron, heavy hole, light hole, and spin–orbit-splitting hole, respectively. Equation (14) is a system of four equations for five parameters a, b, c, d, e. Besides equations (14), we have the additional condition $e/c = 3/2$, which corresponds to the ratio of the matrix element of the (3/2; 1) band to those of the higher conduction bands (5/2; 2) and (3/2; 2). Putting $a = 2b$, $e = (3/2)c$, and $d = (5/2)c$, we obtain the equations in reference [2].

It is easy to see that the spectrum of heavy holes is defined on the basis of the following conditions:

$$f_0^{\pm} = f_3^{\mp} = 0$$

from which we obtain the following condition connecting f_1 and f_2:

$$\left[\frac{\mathrm{d}}{\mathrm{d}r} + \frac{5 \pm (l_0 + \frac{1}{2})}{2r}\right] f_{2,k_h}^{\pm} + \frac{\sqrt{3(l_0 + \frac{3}{2})(l_0 - \frac{1}{2})}}{2r} f_{1,k_h}^{\pm} = 0. \tag{15}$$

Similarly, the spectrum (13) leads to a condition:

$$\left[\frac{\mathrm{d}}{\mathrm{d}r} + \frac{1 \mp (l_0 + \frac{1}{2})}{2r}\right] f_{1,k_h}^{\pm} + \frac{\sqrt{3(l_0 + \frac{3}{2})(l_0 - \frac{1}{2})}}{2r} f_{2,k_h}^{\pm} = 0. \tag{16}$$

Using (15), from our equation system, we find the solution through the cylindrical Bessel function:

$$f_{2,k_h}^{\pm} = \frac{I_{l_0+1/2\pm1/2}(k_h r)}{r^{3/2}}. \tag{17}$$

And using (16), we find the following solution:

$$f_{1,k}^{\pm} = \frac{I_{l_0+1/2\pm1/2}(kr)}{r^{3/2}}. \tag{18}$$

The other functions are expressed through (17) or (18) with the use of (15) or (16), as well as by equations (1)–(9). Thus, we find

$$f_0^{\pm}(kr) = \frac{\sqrt{2}r\mathrm{i}E}{\alpha(E - E_g)} \frac{\frac{a}{2}\left[1 - \frac{6e^2k^2}{E(E - E_0 - \Delta_0)}\right] + \left[bcd - \frac{ac^2}{8}\right]\frac{k^2}{E(E - E_0)}}{\left[\frac{cd}{E - E_0} + \frac{ab}{E - E_g}\right]} f_1^{\pm}(kr) \tag{19}$$

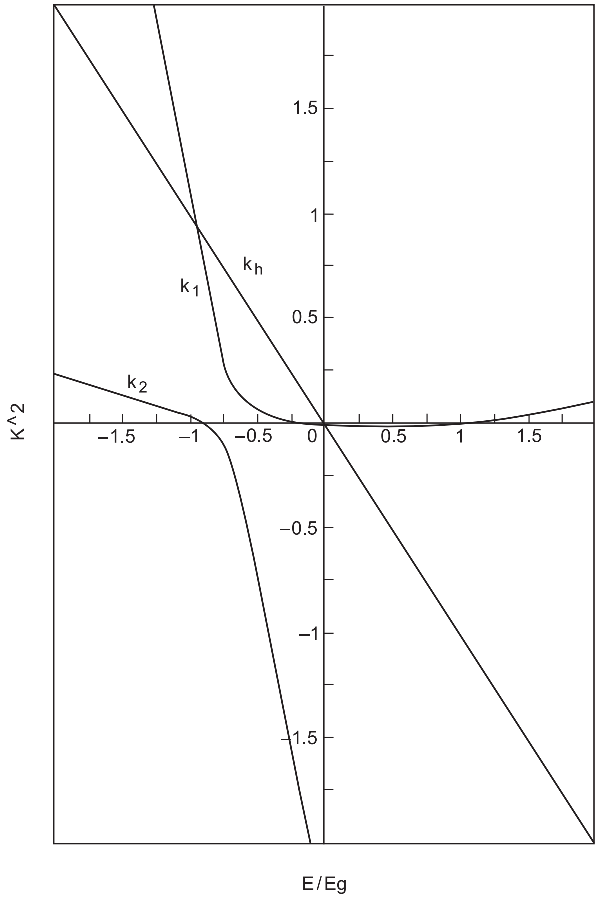

(a)

Figure 2. The solutions of the biquadratic equation (13) as functions of energy for InAs (a) and HgTe (b).

$$f_3^{\mp}(kr) = \mp\frac{2\mathrm{i}(E-E_g)}{ak}\frac{1-\dfrac{k^2}{E}\left[\dfrac{6e^2}{E-E_0-\Delta_0}+\dfrac{c^2/4}{E-E_0}+\dfrac{2b^2}{E-E_g}\right]}{1-\dfrac{6e^2k^2}{E(E-E_0-\Delta_0)}+\left(\dfrac{2bcd}{a}-\dfrac{c^2}{4}\right)\dfrac{k^2}{E(E-E_0)}}f_0^{\pm}(kr). \tag{20}$$

The boundary conditions requiring the equality of radial function to zero on a quantum dot boundary have the following form:

$$\begin{aligned} &C_1^{\pm} f_1^{\pm}(k_1r) + C_2^{\pm} f_1^{\pm}(k_2r) + C_3^{\pm} f_1^{\pm}(k_hr) = 0 \\ &C_1^{\pm} f_2^{\pm}(k_1r) + C_2^{\pm} f_2^{\pm}(k_2r) + C_3^{\pm} f_2^{\pm}(k_hr) = 0 \\ &C_1^{\pm} f_3^{\pm}(k_1r) + C_2^{\pm} f_3^{\pm}(k_2r) = 0 \end{aligned} \tag{21}$$

where $k_{1,2}$ are the solutions of the biquadratic equation (12). In figure 2 the solutions $k_{1,2}$ as functions of energy for the InAs (figure 2(a)) and HgTe (figure 2(b)) cases are shown.

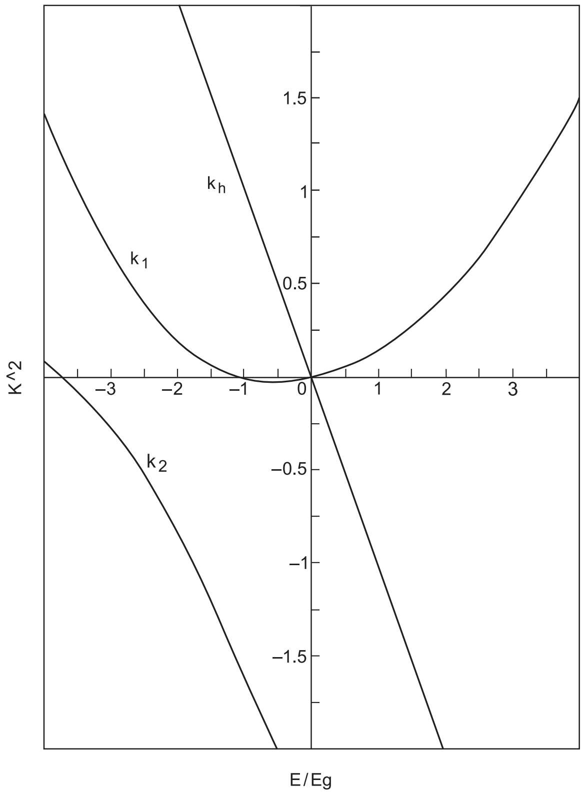

(b)

Figure 2. (Continued)

The spectrum of the charge carriers in a quantum dot is defined from the equality to zero of a determinant of the system (19).

Using the relations for Bessel functions, we can write the system of equations (19) in the form

$$C_1^{\pm}\left[J_{l_0+1\pm 1/2}(k_1 r) + J_{l_0-1\pm 1/2}(k_1 r)\right] + C_2^{\pm}\left[J_{l_0+1\pm 1/2}(k_2 r) + J_{l_0-1\pm 1/2}(k_2 r)\right]$$
$$- \frac{C_3^{\pm}}{\sqrt{3(l_0+3/2)(l_0-1/2)}}$$
$$\times \left[(2\mp 1)\left(\frac{1}{2}-l_0\right)J_{l_0+1\pm 1/2}(k_h r) + (2\pm 1)\left(\frac{3}{2}+l_0\right)J_{l_0-1\pm 1/2}(k_h r)\right] = 0 \qquad (22a)$$

$$\frac{C_1^{\pm}}{\sqrt{3(l_0+3/2)(l_0-1/2)}}\left[(2\pm 1)\left(\frac{3}{2}+l_0\right)J_{l_0+1\pm 1/2}(k_1 r) + (2\mp 1)\left(\frac{1}{2}-l_0\right)J_{l_0-1\pm 1/2}(k_1 r)\right]$$
$$+ \frac{C_2^{\pm}}{\sqrt{3(l_0+3/2)(l_0-1/2)}}$$
$$\times \left[(2\pm 1)\left(\frac{3}{2}+l_0\right)J_{l_0+1\pm 1/2}(k_2 r) + (2\mp 1)\left(\frac{1}{2}-l_0\right)J_{l_0-1\pm 1/2}(k_2 r)\right]$$
$$+ C_3^{\pm}\left[J_{l_0+1\pm 1/2}(k_h r) + J_{l_0-1\pm 1/2}(k_h r)\right] = 0 \qquad (22b)$$

$$C_1^{\pm}\left[1-\frac{E}{k_1^2}\left(\frac{6e^2}{E-E_0-\Delta_0}+\frac{c^2/4}{E-E_0}+\frac{2b^2}{E-E_g}\right)\right]J_{l_0\mp 1/2}(k_1r)$$
$$+C_2^{\pm}\left[1-\frac{E}{k_1^2}\left(\frac{6e^2}{E-E_0-\Delta_0}+\frac{c^2/4}{E-E_0}+\frac{2b^2}{E-E_g}\right)\right]J_{l_0\mp 1/2}(k_2r)=0 \tag{22c}$$

where the $J_\nu(kr)$ are the spherical Bessel functions.

The system of equations (22) is similar to a system (9) from reference [2]. However, here the nonparabolicity of the spectrum of light holes and electrons, as well as the additional independent parameters determining the electron and spin–orbit-splitting valence band spectra are included. The radial functions $f_1^{\pm}$ and $f_2^{\pm}$ are linear combinations of the radial functions $R_{h1}^{\mp}$ and $R_{h2}^{\mp}$ in [2]. For narrow-gap semiconductors, our results coincide with results obtained in [4], but we also consider the case of HgTe-type zero-gap semiconductors.

The quantum size levels are found from the dispersion equation:

$$\begin{aligned}
&\left[1-\frac{E}{k_1^2}\left(\frac{6e^2}{E-E_0-\Delta_0}+\frac{c^2/4}{E-E_0}+\frac{2b^2}{E-E_g}\right)\right]J_{l_0\pm 1/2}(k_1r)\\
&\quad\times\left[\frac{2\mp 1}{2\pm 1}\frac{l_0-1/2}{l_0+3/2}J_{l_0+1\pm 1/2}(k_hr)J_{l_0-1\pm 1/2}(k_2r)\right.\\
&\quad\left.+J_{l_0+1\pm 1/2}(k_2r)J_{l_0-1\pm 1/2}(k_hr)\right]\\
&\quad-\left[1-\frac{E}{k_1^2}\left(\frac{6e^2}{E-E_0-\Delta_0}+\frac{c^2/4}{E-E_0}+\frac{2b^2}{E-E_g}\right)\right]J_{l_0\pm 1/2}(k_1r)\\
&\quad\times\left[\frac{2\mp 1}{2\pm 1}\frac{l_0-1/2}{l_0+3/2}J_{l_0+1\pm 1/2}(k_hr)J_{l_0-1\pm 1/2}(k_2r)\right.\\
&\quad\left.+J_{l_0+1\pm 1/2}(k_2r)J_{l_0-1\pm 1/2}(k_hr)\right]=0.
\end{aligned} \tag{23}$$

The upper signs correspond to the odd solutions and the lower ones to the even solutions. Note that equation (23) describes the spectrum of free carriers in quantum dots based on narrow-gap semiconductors of InAs type as well as those for free carriers in quantum dots based on semiconductors with zero gap and inverted semiconductors of the HgTe and $Hg_{1-x}Cd_xTe$ types.

In figure 3 the energy of free carriers in a semiconductor quantum dot as a function of the quantum dot radius is shown for InAs (figure 3(a)) and HgTe (figure 3(b)). Curves 1c, 2c and 1v, 2v, 3v correspond to the lowest odd-size levels of the conduction and valence bands. The following band parameters have been used for InAs: $E_g = 0.42$ eV, $\Delta = 0.38$ eV, $m_c = 0.023m_0$, $m_{hh} = 0.4m_0$, $m_{lh} = 0.025m_0$, $m_{sh} = 0.15m_0$; and for HgTe: $E_g = 0.28$ eV, $\Delta = 1.05$ eV, $m_c = 0.03m_0$, $m_{hh} = 0.44m_0$, $m_{lh} = 0.032m_0$, $m_{sh} = 0.15m_0$.

In figure 4 the dependences of the transitions between the first size levels of the valence and conduction bands on the quantum dot radius are shown.

According to Gelfand *et al* [6], the solution of the system of equations in spherical coordinates has the form

$$\Psi_{l_0}^{\tau} = f_{lm\tau}^{l_0}(\tau)T_{mn}^{l_0}\left(\frac{\pi}{2}-\varphi,\theta,0\right) \tag{24}$$

where $T_{mn}^{l_0}$ are generalized spherical functions, $l_0 \geqslant l$, and $-l_0 \leqslant m, n \leqslant l_0$. For $l_0 = 1/2$, the functions $f_1^{\pm}$, $f_4^{\pm}$, and $f_5^{\pm}$, for which $m = \pm 3/2$, $\pm 5/2$, and $\pm 3/2$ respectively, do not give the complete contributions to the wave function. The solutions for the heavy hole are absent.

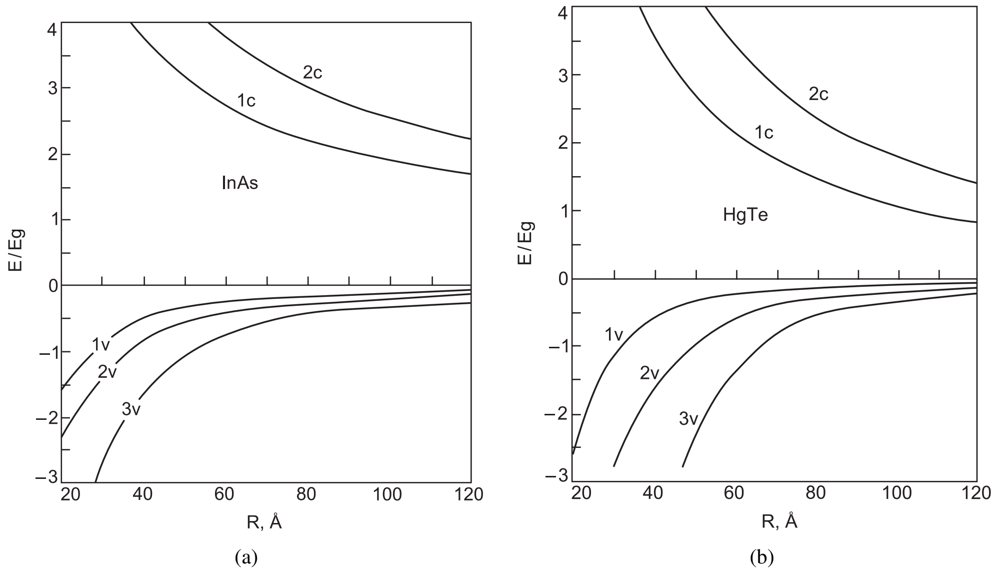

Figure 3. The dependence of the lowest quantum size levels in InAs (a) and HgTe (b) quantum dots as functions of the quantum dot radius.

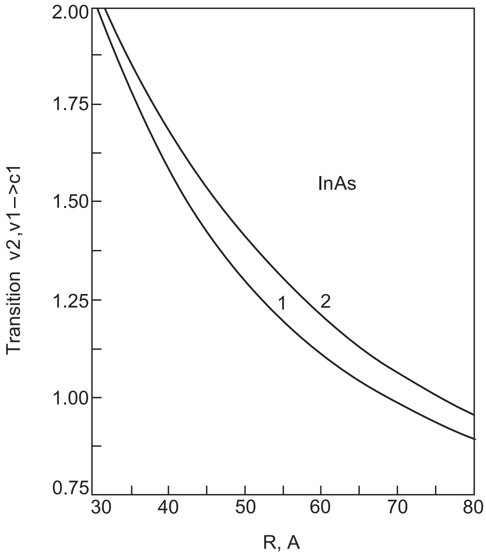

Figure 4. Energies of allowed transitions as functions of the quantum dot size for InAs.

These are the solutions for light holes, electrons, and holes of the spin–orbit-splitting band for which $m = \pm 1/2$. For them, the dispersion equations have the form

$$J_{3/2\pm 1/2}(k_1 r) J_{1/2\mp 1/2}(k_2 r) \left[1 - \frac{E}{k_1^2}\left(\frac{6e^2}{E - E_0 - \Delta_0} + \frac{c^2/4}{E - E_0} + \frac{2b^2}{E - E_g}\right)\right]$$
$$- J_{3/2\pm 1/2}(k_1 r) J_{1/2\mp 1/2}(k_2 r)$$
$$\times \left[1 - \frac{E}{k_2^2}\left(\frac{6e^2}{E - E_0 - \Delta_0} + \frac{c^2/4}{E - E_0} + \frac{2b^2}{E - E_g}\right)\right] = 0. \quad (25)$$

4. Conclusions

In [3–5], the nonparabolicity of the spectra of electrons for GaAs/AlGaAs and InAs/GaSb quantum dots is taken into account. The nonparabolicity is essential for the InAs quantum dot. On the other hand, the necessity for accounting for the influence of the spin–orbit splitting of the valence band on the spectrum of charge carriers in a semiconductor quantum dot has been mooted [2]. In the case of InAs, for which $E_g \approx \Delta \approx 0.4$ eV, both factors are important. Therefore, equations (23) obtained in this work allow one to describe correctly both the situation of a semiconductor quantum dot with normal structure (for example, InAs) and that of a quantum dot based on a semiconductor with inverted band structure (for example, HgTe or $Cd_{1-x}Hg_xTe$ ($x < 0.16$)).

References

[1] Ekimov A I, Onushenko A A, Plyuxin A G and Efros Al A 1985 *Sov. Phys.–JETP* **88** 1490–501
[2] Grigoryan G B, Kazaryan E M, Efros Al A and Yazeva T B 1990 *Fiz. Tverd. Tela* **32** 1772–9
[3] Sercel P C and Vahala K J 1990 *Phys. Rev.* B **42** 3690–710
[4] Efros Al L and Rosen M 1998 *Phys. Rev.* **58** 7120–35
[5] Pryor C 1998 *Phys. Rev.* **57** 7190–5
[6] Gelfand I M, Minlos R A and Shapiro Z Y 1958 *Representations of Groups of Rotations and the Lorentz Group* (Moscow: Fizmatgiz)
[7] Lyubarskiy G Y 1957 *Group Theory and its Application in Physics* (Moscow: Fizmatgiz)